DOI: 10.1021/ma901266u

Macromolecules
ARTICLE

Direct Formation of Nanohybrid Shish-Kebab in the Injection Molded Bar of Polyethylene/Multiwalled Carbon Nanotubes Composite

Jinghui Yang, Chaoyu Wang, Ke Wang,* Qin Zhang, Feng Chen, Rongni Du, and Qiang Fu*

Department of Polymer Science and Materials, State Key Laboratory of Polymer Materials Engineering, Sichuan University, Chengdu 610065, People's Republic of China

Received June 12, 2009; Revised Manuscript Received July 5, 2009

ABSTRACT: The formation of a nanohybrid shish-kebab (NHSK) superstructure, in which fibrillous carbon nanotubes (CNTs) act as shish while polymer lamellae act as kebab, is a novel way to bond the polymer and CNTs together and was first observed in the solution crystallization of polyethylene in the presence of CNTs. In this work, a direct formation of nanohybrid shish-kebab in the injection molded bar of high-density polyethylene (HDPE)/multiwalled carbon nanotubes (MWCNTs) composite, has been achieved, via a so-called dynamic packing injection molding technology (DPIM), in which oscillatory shear field was imposed on the gradually cooled melt during the packing solidification stage. Interestingly, whatever the long axis of CNTs is perpendicular to or parallel to the shear flow direction, the lamellae of PE is always perpendicular to long axis of CNTs. The three-step mechanism, including (1) the disentanglement and orientation of both PE and CNTs, (2) PE folded-chain lamellae directly nucleated on CNTs surface and/or first formation of PE extended-chain shish directly on CNTs surface then followed by nucleation of folded-chain lamellae, and (3) the crystallization of PE kebabs on the PE decorated CNTs fibrils, was proposed to understand the formation of NHSK under effect of shear. Importantly, the NHSK structure can bring significant mechanical reinforcement in the HDPE/MWCNTs composite. For the oriented composites containing 5% MWCNTs, its tensile strength is increased by 150% and 270%, compared to the oriented pure HDPE and the isotropic composites containing 5% CNTs, respectively; meanwhile, its Young's modulus is enhanced by 130% and 180%, compared to the oriented pure HDPE and the isotropic composites containing 5% CNTs, respectively. This work is the first to enlarge the theoretical value and application potential of NHSK structure in the crystallizable polymer/CNTs composite.

1. Introduction

Polyolefin is the most common thermoplastic, and it is widely used in the fields of both industry and academe. In recent years, CNTs-reinforced polyolefin composites have attracted intensive interests. In many cases, before melt compounding with polyolefin, surfacial functionalization and grafting modification of CNTs were necessary for ensuring homogeneous dispersion and strong interaction.[1] Blake et al.[2] functionalized multiwalled carbon nanotubes (MWCNTs) using *n*-butyllithium, and then the modified MWCNTs were covalently bonded with chlorinated polypropylene (C-PP). Only addition of 0.6% C-PP grafted MWCNTs into C-PP could improve Young's modulus, tensile strength and toughness for several orders. Gray et al.[3] developed a treatment way to covalently grafted alkyl chain (octadecylamine) on single-walled carbon nanotubes (SWCNTs), enabled SWCNTs hydrophobic to be easily dispersed in polyolefin. In our previous studies,[4,5] octadecylamine-grafted MWCNTs were used to prepare highly oriented PP/MWCNTs composite; low amount of CNTs (0.3%) made a increment of 100% in extension ductility simultaneously a limited promotion in tensile strength and modulus. Yang et al.[6] conducted reactive grafting modification of aminated MWCNTs with maleic anhydride grafted polyethylene (PE) during melt blending; the stiffness, strength, ductility and toughness of PE are all improved by the addition of PE-*g*-MWNTs. Except for functionalized CNTs obtained through grafting modification, the other strategy making CNTs uniformly dispersed in polyolefin is to develop a particular compounding method. Lu et al.[7] obtained an individual dispersion of CNTs in PP using latex technology; Chen et al.[8] prepared ultrahigh molecular weight PE (UHMWPE)/MWCNTs composites by gelation/crystallization from solution; in the study by Zhang et al.,[9] a good CNTs dispersion was achieved by spraying an aqueous solution of SWNTs directly onto a fine UHMWPE powder.

For the strategies demonstrated above, their processed procedures are complicated, and the production efficiency is very low, which made these strategies unsuitable for abundant manufacture of polyolefin/CNTs composites. However, an argument has arisen whether good dispersion and strong interfacial adherence can be achieved directly through melt compounding of polyolefin and pristine CNTs (or by a simple purified treatment by the mixing acid solution). For some polar polymers, such as nylon 6,[10] simple melt compounding could indeed induce uniform dispersion and good compatibility of CNTs in nylon 6, thus resulting in prominent mechanical enhancement. Nevertheless, for nonpolar, hydrophobic polyolefin, although in some cases directly melt compounding CNTs with polyolefin could also achieve a good dispersion, the mechanical reinforcement in these composites is not as good as expected. For example, in the PE/MWCNTs composites prepared through melt blending in an extruder,[11] the flexibility and break strength were continuously decreased with increasing CNTs loading; for the injection-molded bars of a PP/MWCNTs composite,[12] when the CNTs content was increased up to 5%, the increment was only 20% for yield stress while being 40% for Young's modulus; in the study by Xiao et al.,[13] the Young's modulus and tensile strength of low

*Corresponding authors. Telephone: 0086-28-85405402. E-mail: qiangfu@scu.edu.cn (Q.F.); wkestar@scu.edu.cn (K.W.).

 Published on Web 07/17/2009

density PE (LDPE)/MWCNTs composite were promoted by 89% and 56%, respectively, when the CNTs content reached a high value (10 wt %). Obviously, the interfacial adhesion of the polyolefin/CNTs composites prepared by direct melt blending should be improved to generate efficient stress transfer from matrix to filler, thus obviously elevating the reinforcement efficiency of CNTs.

It is well-known that CNTs could act as an efficient nucleating for some crystallizable polymers.[14−16] Therefore, crystalline polymer chains can deposit on the CNTs surface through the driving force of epitaxial crystallization. In particular, a novel nanohybrid shish-kebab (NHSK) superstructure, in which fibrillous CNTs act as shish while polymer lamellae as kebab, has been observed in the solution crystallization of polyethylene in the presence of CNTs, and it likely follows the "size-dependent soft epitaxy" mechanism, as first suggested by Li et al.[17] By far, the most-reported method used to obtain a fine NHSK superstructure of polymer/CNTs involved the strict procedure of solution crystallization. Li et al.[18] maintained the crystalline temperature of polymer/CNTs/xylene suspension as constant for a long time to prepare NHSK in PE/CNTs and nylon-6,6/CNTs solution. Xu et al.[19] varied the solubility of PE in xylene through incorporation of supercritical CO_2 and made PE chains deposited and crystallized on CNTs to obtain well-defined NHSK. Zhang et al.[20] sprayed the aqueous solution of SWNTs directly onto the fine UHMWPE powder and then melt compounded the CNTs-coated PE and extrusion-stretched into a sheet, where the NHSK structure of UHMWPE/SWNTs was found. Contrasting to the covalently functionalized method of grafting modification, the formation of NHSK is regarded as a noncovalently functionalized method used to alter the surface properties of CNTs through wrapping by polymer lamellae and as a novel method to bond the polymer and CNTs together. It is important and significant that in situ formation of NHSK superstructure in polymer/CNTs composites is used instead of in solution formation to enhance the interfacial adhesion between polymer and CNTs, thus efficiently improving the mechanical properties. However, to the best of our knowledge, there is no research concerning: (1) the preparation of the NHSK structure directly through melt compounding and (2) evaluating the effect of the NHSK structure on mechanical reinforcement of polyolefin/CNTs composite.

In our previous work,[21,22] the injection-molded bar containing the NHSK structure was first prepared by incorporation of tiny-rod shaped inorganic whiskers into high density PE (HDPE). The structural character of NHSK is dramatically affected by the molecular weight of HDPE; meanwhile, the structural perfection of NHSK plays a positive role in the mechanical enhancement. Obviously, in the academic investigation field, CNTs receive more attention than inorganic whisker, and the polymer/CNTs composite has a huge potential for application in industrial manufacture. However, in the published literature, the prepared NHSK samples of polymer/CNTs were individual entities and were not compounded into a polymer matrix. Forming a large scale NHSK composite is important to bringing the NHSK structures to real applications. The major aim in this study is to prepare a fine NHSK structure of HDPE/MWCNTs directly through injection molding processing without any surface functionalized treatment on MWCNTs. In order to optimize structural orientation and facilitate nucleation and crystallization of HDPE, a so-called dynamic packing injection molding technology (DPIM) was adopted, in which an oscillatory shear field was imposed on the gradually cooled melt during the packing solidification stage. A direct formation of NHSK structure in the injection molded bar of high-density polyethylene (HDPE)/multiwalled carbon nanotubes (MWCNTs) composite has been achieved for the first time in our work. It is anticipated that this work will open a novel, convenient gateway to achieving a well-defined NHSK structure directly in injection-molded processing, offering potential for practical application and enlarging the theoretical merit of the NHSK structure in the crystallizable polymer/CNTs composite.

2. Experimental Section

2.1. Materials and Preparation of Composite. High density polyethylenes (HDPE), with a trade name 2911, was used as the matrix. It had a melt flow index of 20 g/10 min and molecular weight (M_w) of 1.2×10^5, and it was supplied by Fushun Petrochemical Corp. Raw MWCNTs was purchased from Shenzhen Nanotechnology Co. Ltd. The main range of diameter of the raw MWCNTs was about 10−20 nm and their length was about 5−15 μm, the purity was lager than 95%, and ash (catalyst residue) is less than 0.2%. MWCNTs were used without any pretreatment. The contents of MWCNTs are 1%, 3%, 5%, and 7%, respectively.

After being dried in 70 °C for 12 h in a vacuum environment, MWCNTs were blended with HDPE using a corotating twin-screw extruder (TSSJ-25) with a barrel temperature of 150 °C. After being pelletized and dried, the blends were injected into a mold with aid of a SZ 100 g injection molding machine with a barrel temperature of 180 °C and injection pressure of 900 kg cm-2. In order to prepare materials containing highly oriented shish-kebab structure, special molded equipment named as dynamic packing injection molding (DPIM) was attached on the injection machine. The processing parameters and the characteristics and detail experiment procedure of DPIM were described elsewhere.[23,24] The major feature of DPIM is that the melt is first injected into the mold then forced to move repeatedly in a chamber by two pistons that moved reversibly with the same frequency as the solidification progressively occurs from the mold wall to the molding core part.

2.2. Characterizations and Measurement. CMT4104-SANS was used to test the tensile properties under a crosshead speed of 50 mm/min according to GB/T1040−92 standard, and the measured temperature was around 25 °C. At least five samples have been measured and the average values were reported.

A polarized light optical microscope equipped with a hot stage was used to study the nonisothermal crystallization morphology and dispersion of composites. The samples sandwiched between two microscope coverslips were first heated to 150 °C, then cooling to 100 °C at a rate of 5 °C/min. The crystallization process was observed and the morphologies were recorded by taking photographs at constant time intervals.

A Perkin-Elmer diamond-II differential scanning calorimetry (DSC) was used to determine the melting and crystallization behaviors of the injection-molded specimen. The injection-molded specimens (about 5 mg) were heated from 20 to 170 °C at a heating rate of 10 °C/min under a nitrogen atmosphere, holding at 170 °C for 5 min and followed by cooling to 20 °C at a rate of 10 °C/min. After nonisothermal crystallization measurement, a second melting process was performed from 20 to 170 °C at a heating rate of 10 °C/min.

The morphologies of the blends were studied via SEM. After fractured parallel to flow direction in liquid nitrogen, the specimens were etched and extracted out from the surface of cryo-fractured bar by using the mixing acid solution.[25] Finally the surfaces were covered with a thinLayer of gold, the crystalline morphology was observed by a SEM instrument (Inspect F, FEI company) operation at 20 kV.

The rheological measurements were performed on a controlled strain rheometer (Malvern Instruments Ltd., U.K.) with a frequency range of 0.03−100 rad/s using 2.5 cm diameter parallel plates at 170 °C. Testing sample disks with a thickness of 1.5 mm and a diameter of 2.5 mm were prepared by compression-molding of the extruded pellets at 170 °C for 3 min.

3. Results and Discussion

3.1. Dispersion of MWCNTs. The dispersion of MWCNTs in HDPE matrix is estimated by visual analysis, PLM and

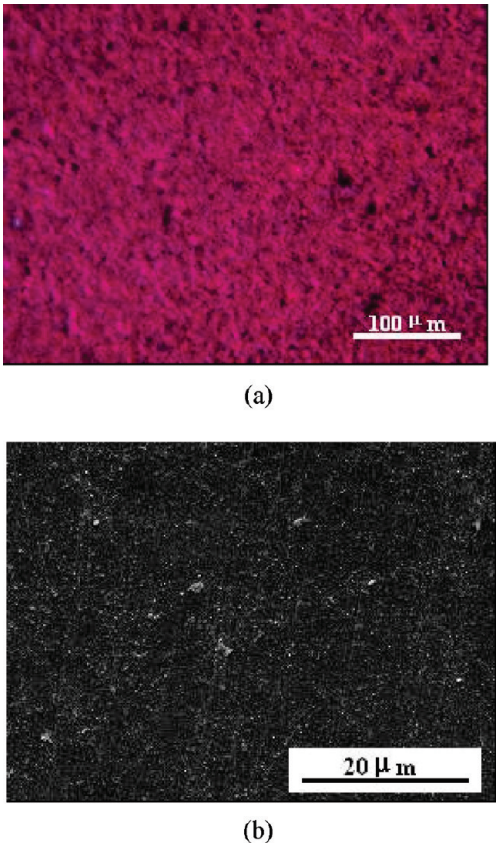

Figure 1. Dispersion of CNTs in the injection-molded bar of composite characterized by (a) PLM and (b) SEM (the content of CNTs is 5%).

SEM (Figure 1), and indirect analysis, melt rheometry (Figure 2). PLM observation is used to distinguish the particles of MWCNTs aggregation with size of several micrometers within a large inspected area, as shown in Figure 1a. In the composite containing 5 wt % MWCNTs, the amount of micrometer-scale aggregation of CNTs is less, implied that a majority of CNTs exists as a fashion with smaller size-scale. As being observed from the SEM micrograph of Figure 1b, numerous tiny units of CNTs with size-scale of hundred nanometers are dispersed in HDPE matrix uniformly. Therefore, a relative good state of CNTs dispersion in HDPE can be achieved merely through direct melt blending of HDPE and MWCNTs, most likely due to the low molecular weight of HDPE used in our experiment. Due to the reliability and veracity of melt rheological analysis on estimation of CNTs dispersion behavior in polymer melt as approved by many published studies,[9,26] the overall dispersion state of CNTs is further demonstrated upon a viewpoint of viscoelasticity, as presented in Figure 2, parts a (elastic modulus G' vs shear frequency) and b (viscous modulus G'' vs shear frequency). As increasing MWCNTs content from 1 to 7 wt %, the viscoelastic moduli within whole frequency range are promoted continuously. In particular, a plateau of G' within low frequency regime appears when the CNTs content is elevated from 3 to 5 wt %, which implied a percolation network of CNTs formed at 5 wt % CNTs, and the relaxation and mobility of PE chains are restricted dramatically by geometric confinement effects of CNTs.[26] The occurrence of percolation threshold at 3 wt % CNTs loading also suggests the overall good dispersion of CNTs in HDPE matrix. Moreover, it should be noted that the change of rheological properties is not obvious when the CNTs content increases from 5 wt % to 7 wt %. This means the uniform dispersion of

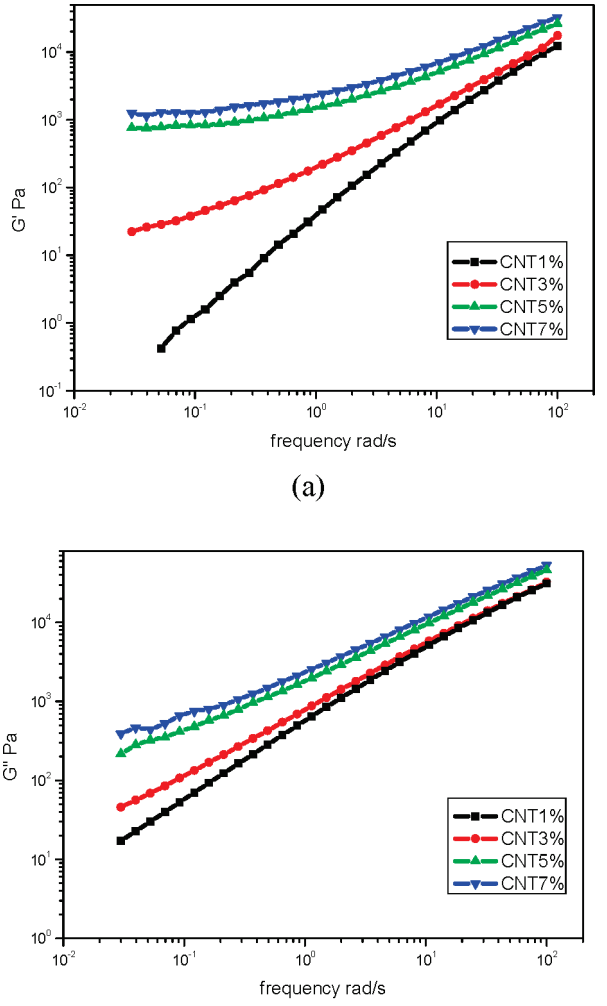

Figure 2. Viscoelastic properties of HDPE/MWCNTs composites with different CNTs contents: (a) elastic modulus G' vs ω (b) viscous modulus G'' vs ω.

CNTs will approach a saturation state after the CNTs content reaches 5 wt %; addition of more amounts of CNTs may possibly make severe aggregation of CNTs in HDPE.

3.2. NHSK Superstructure in Injection-Molded Composite. To distinguish the crystalline structure in the injection-molded bar clearly, the amorphous phase of HDPE has been chemically etched and extracted out from the surface of the cryo-fractured bar by using the mixing acid solution. Macroscopically, the main feature of DPIM samples is the shear-induced morphologies with the core in the center, oriented zone surrounding the core and the skin layer in the cross-section areas of the samples. As example, some typical SEM images of crystalline structure for both pure HDPE and composite with 5 wt % CNTs are presented in Figure 3, these micrographs are acquired at a depth about 400 μm to the outmost surface of the injection-molded bar. The SEM image of Figure 3a shows highly ordered alignment of lamellae in the bar of pure HDPE prepared by DPIM. The thickness direction (c-axis) of the PE lamellae is approximately parallel to the shear flow direction; correspondingly, the lateral direction (a-axis) perpendicular to the flow direction. From Figure 3a, it is hard to distinguish the shish-kebab entity clearly in pure HDPE, since only a few thin shish could be seen faintly in the bottom-right part of this figure. The composite containing 5 wt % CNTs is chosen as the representation for

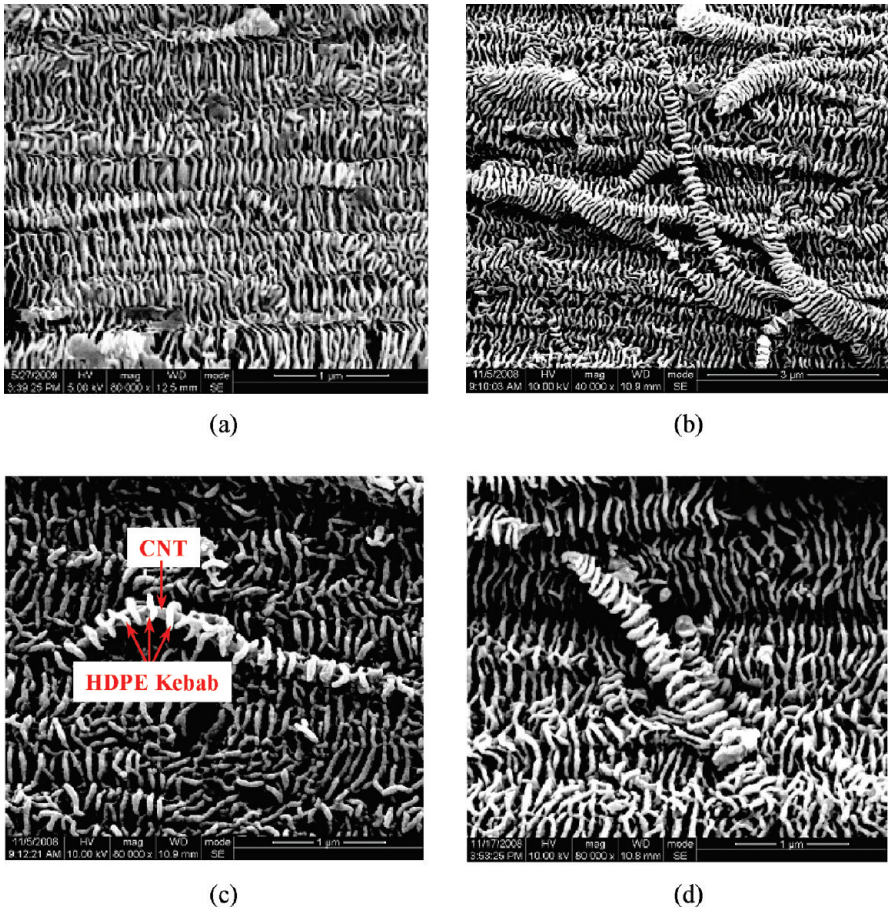

Figure 3. Crystalline morphologies in the DPIM bars of (a) pure HDPE, magnification of 80 000×, (b) composite with 5% CNTs, magnification of 40 000×, and (c and d) composite with 5% CNTs, magnification of 80 000× (the shear flow direction is horizontal).

a series of composites with different contents of CNTs, to ascertain the detail crystalline structure in the injection-molded bar. The most interesting finding about crystallographic structure is the in situ formation of well-defined NHSK crystal in the injection-molded composite, as shown in Figure 3b. In the SEM image of Figure 3b with relatively low magnification (40 000×), tens of NHSK crystals can be observed distinctly; the longitudinal direction (the long axis of CNTs) of NHSK crystal is not always parallel to the shear flow direction. The image of Figure 3c with relativelt high magnification (80 000×) presents the long axis of NHSK aligning approximately parallel to the flow direction, while Figure 3d (magnification of 80 000×) shows the long axis of NHSK inclining away from the flow direction. However, whether the long axis of CNTs is perpendicular to or parallel to the shear flow direction, the lamellae of PE are always perpendicular to the long axis of CNTs, indicating a strong epitaxy growth of PE on the surface of CNTs under shear effect. It should be noted that the observed PE crystal thickness is in the range 40−70 nm, which is too high compared with the known value, and it is probably due to the Au coating in the SEM sample preparation process. Since pure HDPE can also form the shish-kebab structure under shear, the key in our work is to verify that, in HDPE/CNT blends, the shish-kebab formed have MWCNTs as the shish. By carefully examining Figure 3, parts a to d, in detail, one may identify some structural features of NHSK significantly differing from the PE matrix shish-kebab. The diameter of the shish in NHSK is prominently thicker than pure PE shish consisting of extended PE chains (seen in Figure 3a). Otherwise, the length of kebab on NHSK is remarkably shorter than PE matrix lamellae. On the NHSK entities, bended lamellae wrapped around thick thread can be observed unambiguously. These structural characters may aid one to distinguish NHSK entity from PE matrix shish kebab easily. It is reasonable to assume that CNT serves as the shish due to the heterogeneous nucleation effect, however, it is not clear at this moment if there are 100% CNT in the shish. Also the formation of NHSK in the injection molded depends on the position along sample thickness, as a result of different flow and thermal conditions. The hierarchy structure and orientation structure of the samples along the direction of sample thickness from skin and core were carefully characterized. SEM images illustrated crystalline structure at different zones of the DPIM bar of the composite with 7% CNTs are presented in Figure 4. In all zones, the depth ranged from 50 to 1500 μm, and the NHSK entity can be detected. Obviously, the crystalline morphology differences among different zones originated from the interplay of shearing and thermal history during the DPIM process. Two issues should be emphasized: (1) although the matrix-oriented feature is weak in the zones of skin (depth of 50 μm) and core (depth of 1500 μm), a NHSK superstructure can also be formed, and (2) the aligned directions of NHSK entities are not identical in different zones. The reason why the NHSK entities align in different directions will be discussed in section 3.4. These observations verify again that a strong heterogeneous nucleation effect of CNTs can cause a NHSK superstructure to exist during an intensive shearing process.

3.3. Calorimetric Analysis. The DSC melting curves of the DPIM bars of HDPE/CNTs composites with different CNTs contents (0−7 wt %) are represented in Figure 5a. A double-melting behavior is detected for all samples. The first melting peak for the pure HDPE, around at 132.5 °C, is

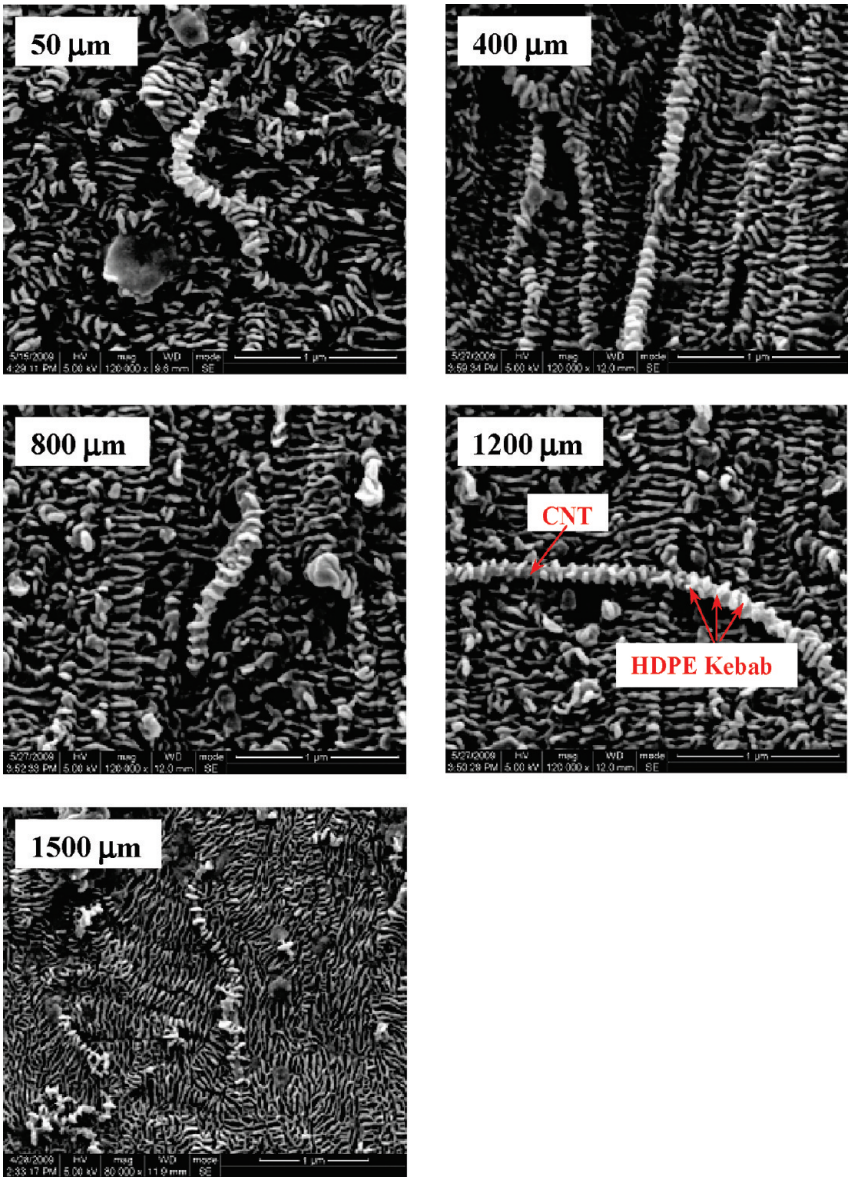

Figure 4. Crystalline morphologies of different zones in the DPIM bar of composite with 7% CNTs, the numbers in micrograph indicate the depth from the outmost surface of injection-molded bar (the shear flow direction is vertical).

denoted to melting of folded-chain lamellae. With increasing CNTs from 1% to 7%, a decrease in the first melting peak for about 1.5 °C can be detected, indicating that the thickness of folded chain lamellae is somewhat altered as incorporation of CNTs takes place. The geometric confinement effect of CNTs can break the continuity of the polymer matrix and hinder PE chain motions to form thick lamellae.[27] For all samples, the second melting peak is higher than the first melting peak by about 4.5 °C. A phenomenon should be noted that the intensity of the higher melting point peak is significantly weak for the pure HDPE comparing to the composites with CNTs. This indicates that incorporation of CNTs has facilitated the formation of crystalline fraction with high melting point. Several factors could be contributed to the upshift of the melting temperature: the formation of thicker lamellae, or confined crystals in a nanoenvironment, or simply the favorable interaction between the PE chains and the MWNT surfaces. However, for polyethylene, the temperature of 4.5 °C higher than the first melting peak is usually considered as due to the melting of extended-chain crystalline structure, as in the case of polyethylene crystallized under high pressure.[28,29] If it is the case, our result indicates that incorporation of CNTs has caused an easier formation of PE shishs and/or probably extended-chain PE layer, which are wrapped around CNT shish. After eliminated thermal history of the injection molded samples at 170 °C, the nonisothermal crystallization was subsequently implemented, as shown in Figure 5b. As increasing the CNTs content from 0 to 7%, the cooling crystallization temperature (T_c) is continuously promoted from 118 to 123.5 °C. In particular, only addition of 1% CNTs into HDPE can elevate the T_c to 122 °C, denoting the efficient heterogeneous nucleation of CNTs for facilitating PE crystallization. The second melting measurements were performed after nonisothermal crystallization process, as shown in Figure 5c. The high temperature melting peak disappears totally for all samples, indicating extended-chain crystalline structure can not be generated from isotropic melt though heterogeneous nucleation effect of CNTs is still present. Obviously, oscillatory shearing during DPIM process plays a crucial role on the formation of extended-chain crystalline fraction of PE. To obtain more information about the crystalline characters

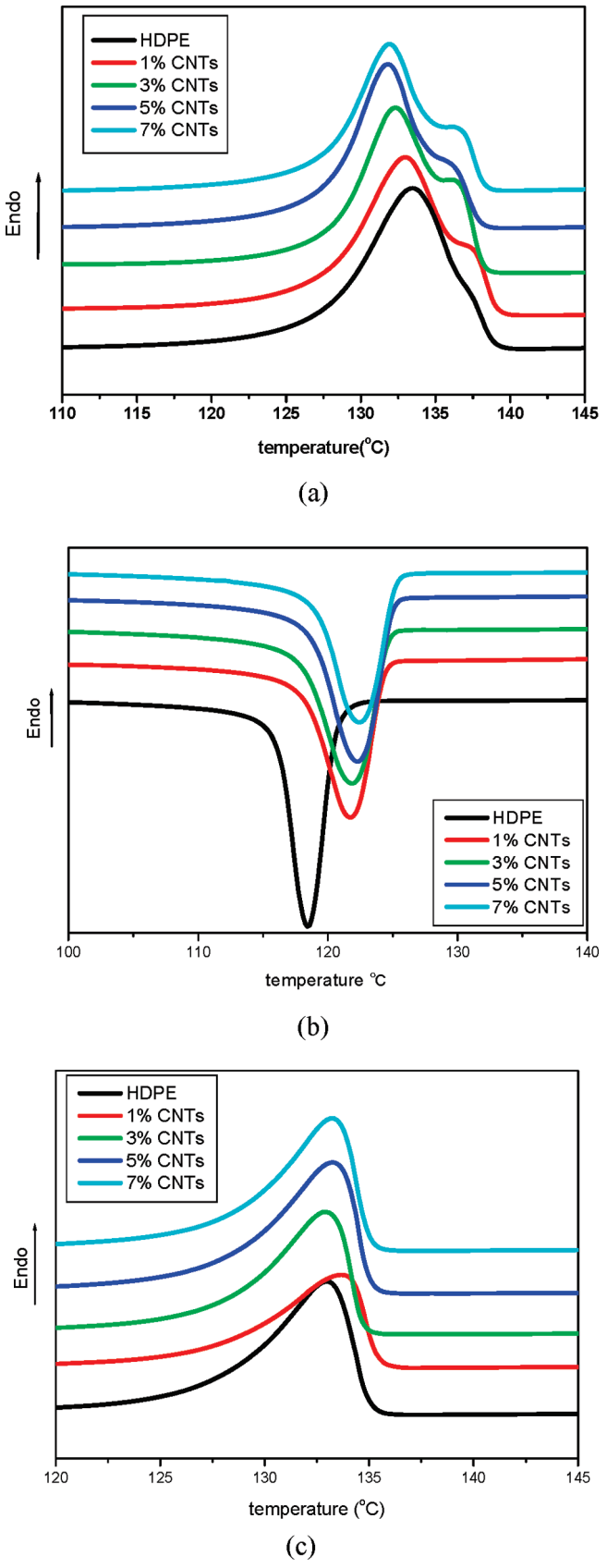

Figure 5. DSC thermograms of composites with different CNTs contents: (a) melting, (b) cooling crystallization, (c) second melting.

from calorimetric data, a quantitative comparison of relative crystallinity (X_c) between first heating and second heating should be done. The heats of fusion can be achieved through integrating area of molten peak, then these heats of fusion are divided to the fusion of HDPE with 100% crystallinity as 293.6 J/g[30] to calculate relative crystallinity. For the first heating process, the crystallinities are 67.8, 69.6, 70.8, 65.4 and 67.8%, corresponding, respectively, to 0, 1, 3, 5 and 7% CNTs. The crystallinities are comparative between pure HDPE and composites. In the second heating process, the X_c of pure HDPE does not significantly change, which is 66.2%; whereas for the composites with CNTs, the crystallinities are 60.3, 59.4, 62.3, and 59.4%, corresponding respectively to 1, 3, 5, and 7% CNTs, so an obvious reduction of X_c (8−10%) can be detected except for 5% CNTs. Comparing the crystallinities in second heating process, the X_c of composite is lower than that of pure HDPE, which is accord with the data by Kodjie et al.[27] and attributed to the fact that CNTs can disturb the continuity of polymer matrix, thus resulting in more gain boundaries as well as defects. On the other hand, reduction of X_c for the composites, compared between first/second heating, may be related to the mass fraction of extended chain crystal, because the higher molten peak can not be found in the second heating process. Of course, to exactly prove the formation of extended chain crystals on CNTs surface, a small-angle X-ray experiment should be carried out to achieve further powerful evidence, which is our current effort.

3.4. The Mechanism of NHSK Superstructure Formation under the Effects of Shear. According to the findings of SEM and calorimetry, a hypothetical mechanism about the formation of NHSK superstructure during DPIM process is schematically proposed in Figure 6, and interpreted in detail as the following descriptions. In an initial situation, a bimodel entanglement framework, consisting of two entangled networks for coiled PE chains and bended CNT fibrils, exists in the melt of HDPE/MWCNTs system, as shown in Figure 6a. The shear flow function imported during the DPIM process may disturb the entangled, isotropic networks of both of PE chanis and CNT fibrils. While due to the difference of intrinsic elastibility between PE chain and CNT fibril, the deformation and orientation of CNT fibril differ from that of PE chain, as shown in Figure 6b. The PE chains possess high flexibility to easily take place distanglement and orientation during shear process, and a preferentially oriented direction can be distinctly detected to parallel to the shear flow direction. On the other hand, the CNTs networks have high rigidity and low flexibility. The shear gradient from skin to core in the injection-molded bar only forces the bended, entangled CNTs to extend and disentangle partially, resulting in a limited destruction of the CNTs network. So the orientations of CNT fibrils are random because it is hard for the oscillatory shearing to freely tumble the CNTs with high rigidity and low flexibility; simultaneously, some entanglement sites of CNTs still exist after the shearing process. Subsequently, in Figure 6c, two possible nucleated paths for PE kebab epitaxially crystallized on CNT shish are proposed. For the first nucleated path, CNTs with high nucleation effectivity can attract PE chains deposited on its surface and chain-fold occurs directly on the CNTs surface; correspondingly, the chain-fold direction is perpendicular to the long-axis direction of CNT. In the second nucleated path, the crystallization of the extended-chain PE shish directly on the CNTs surface occurs before the formation of folded-chain lamellae. Whether the oriented direction of CNTs is parallel to the shear direction or not, the formation of extended-chain crystalline regime (shish) directly on CNTs surface is reasonable, using the CNTs as template. Finally, the PE kebabs crystallize and grow on the CNT shish or the PE shish decorated CNT fibrils with their lateral

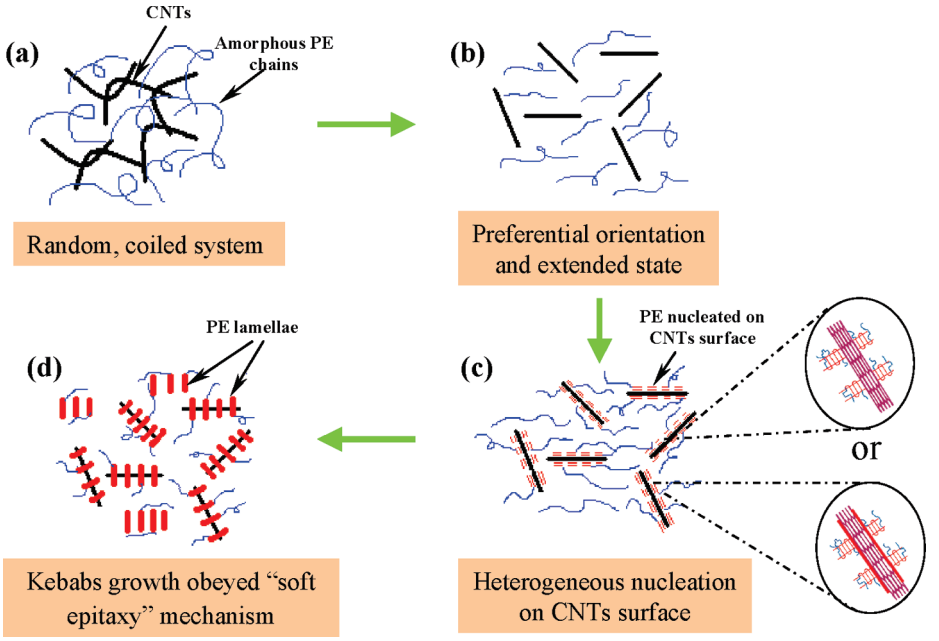

Figure 6. Schematic representations of the hypothetical mechanism of NHSK superstructure formation during the DPIM processing.

direction (*a*-axis) perpendicular to the long axis of CNTs, obeying the "soft epitaxy" crystallization mechanism, as suggested by Li et al.[17] Simultaneously, the framework of orderly arranged PE lamellae forms for the PE matrix fraction, with the *c*-axis of lamellae preferentially parallel to the direction of shear flow, as shown in Figure 6d. It should be noted that the basic assumptions of our model are as follows: (1) the stretched PE chains have higher crystallization capability than the random, coiled ones due to the reduced crystallization barrier after being stretched; (2) the extended PE chains (shish layer), formed around the CNTs surface, is facilitated by the relative "simple" geometric configuration of CNTs, which changed from bended coil to highly extended fibril; (3) the growth direction of kebab (*a*-axis) dominated by arrangement situation of CNTs, exhibited as the *a*-axis of kebab perpendicular to the long axis of CNTs, is consistent with a geometric confinement arrangement, namely the soft epitaxy mechanism.

It should be also noted that the existence of extended-chain crystalline regime covered around CNT fibrils under the effect of shear proposed in our work is somewhat different from that suggested by Li et al.,[14] and it is supported by some experimental evidence as follows: (1) the mass fraction of matrix shish formed in the pure HDPE is quite less; (2) the mass fraction of extended-chain crystalline structure is significantly improved after incorporation of CNTs, and meanwhile, the matrix shish-kebab entity is hard to find in the composite containing CNTs; (3) CNTs possess high nucleation efficiency for facilitating PE crystallization.

3.5. Mechanical Reinforcement by NHSK. It is highly desired that the NHSK superstructure can bring a remarkable mechanical reinforcement in the HDPE/MWCNTs composite. The stress−strain measurements were implemented for the composites containing different contents of CNTs (0−7 wt %). For comparison purpose, two types of injection-molded bar, the oriented bar prepared by DPIM and the isotropic bar prepared by conventional injection, are all inspect. In general, a ductility-to-brittle transition in tensile mechanical behavior may occur when the structural feature is varied from isotropy to anisotropy. The tensile strength in the oriented bar is prominently higher than that in the

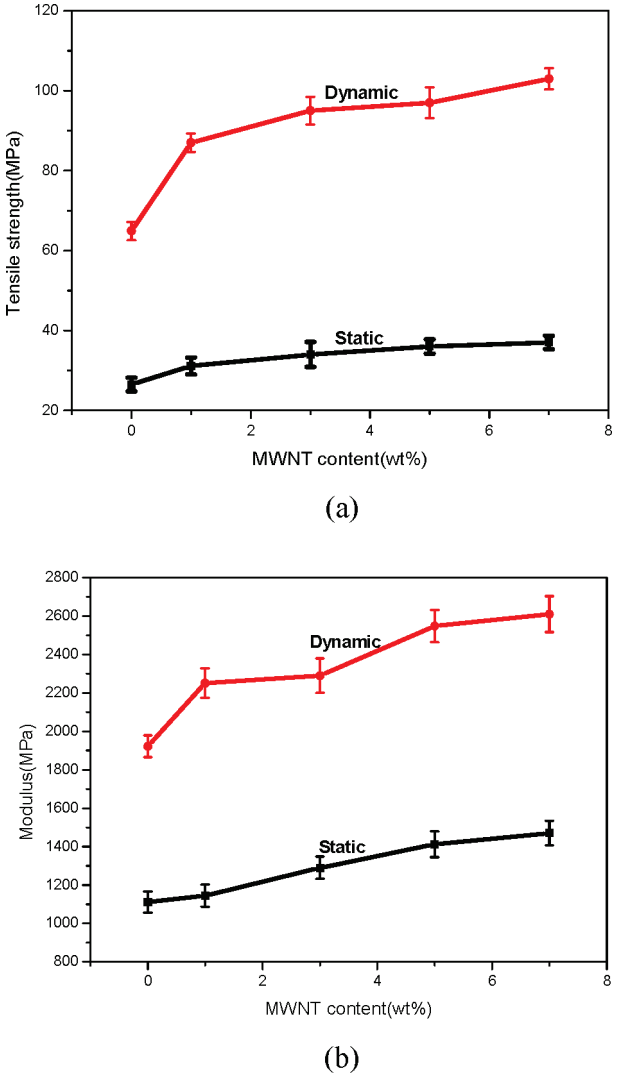

Figure 7. Tensile properties of the composite bars with different CNTs contents: (a) tensile strength; (b) Young's modulus.

isotropic bar, whereas, the ductility of the isotropic bar is obviously better than the oriented one. In order to quantitatively estimate the mechanical reinforcement of injection-molded composite, the values of tensile properties are acquired from the stress−strain measurements. The relations of tensile strength vs CNTs content and Young's modulus vs CNTs content are plotted in Figure 7, parts a and b, respectively. For both oriented sample and isotropic sample, the tensile strength and Young's modulus are all continuously improved with increasing CNTs content. Nevertheless, the reinforcement efficiency by addition of CNTs is more obvious in the oriented sample than in the isotropic sample. The NHSK superstructure formed directly in the injection-molded bar of composite is regarded as an ideal situation for CNTs reinforced polymer. PE kebabs tightly decorated on CNTs shish can significantly enhance the interfacial adhesion and the stress transfer capability between CNTs and PE matrix. For the oriented composites containing 5% MWCNTs, the tensile strength is increased by 150% and 270%, compared to the oriented pure HDPE and the isotropic composites containing 5% CNTs, respectively; meanwhile, the Young modulus is enhanced by 130% and 180%, compared to the oriented pure HDPE and the isotropic composites containing 5% CNTs, respectively. So the NHSK superstructure is indeed efficacious for mechanical reinforcement of the HDPE/MWCNTs composite. However, the increased disentanglement and orientation of CNTs under effect of shear should also contribute, at least in part, to the improvement of mechanical properties. At this moment, it is difficult to separate the contribution of the NHSK superstructure from the disentanglement and orientation of CNTs, since without disentanglement and orientation of CNTs it is not possible to form the NHSK superstructure.

4. Conclusions

The fine nanohybrid shish-kebab superstructure was achieved directly in the injection-molded bar of HDPE/MWCNTs composite prepared by the DPIM technique. In situ formation of NHSK structure in the injection-molding process is attributed to (1) the external shearing effect and (2) the intrinsic crystallization mechanism of soft epitaxy. These two issues cause the preferentially oriented PE chains to form kebabs along the long axis of CNTs shish even when the alignment direction of CNTs is not parallel to the preferentially oriented direction of PE chains. The tensile behavior measurement approved that the NHSK structure brings obvious mechanical reinforcement in the polyolefin/CNTs composite. This work is a preliminary stage for a series of systematic profound investigations concerned preparation of NHSK structure by simple conventional processing method, structural control of NHSK during practical melt compounding process, and NHSK-reinforced polyolefin processing technology.

Acknowledgment. We would like to express our sincere thanks to the National Natural Science Foundation of China for Financial Support (50533050, 20874064, 50873063). The authors gratefully acknowledge the help of Ms. Xinyuan Zhang of the Analytical and Testing Center at Sichuan University for the SEM micrographs.

References and Notes

(1) Hwang, G. L.; Shieh, Y. T.; Hwang, K. C. *Adv. Funct. Mater.* **2004**, *14*, 487.
(2) Blake, R.; Gun'ko, Y. K.; Coleman, J.; Cadek, M.; Fonseca, A.; Nagy, J. B.; Blau, W. J. *J. Am. Chem. Soc.* **2004**, *126*, 10226.
(3) Grady, B. P.; Pompeo, F.; Shambaugh, R. L.; Resasco, D. E. *J. Phys. Chem. B* **2002**, *106*, 5852.
(4) Zhao, P.; Wang, K.; Yang, H.; Zhang, Q.; Fu, Q. *Polymer* **2007**, *48*, 5688.
(5) Hou, Z. C.; Wang, K.; Zhao, P.; Zhang, Q.; Fu, Q. *Polymer* **2008**, *49*, 3582.
(6) Yang, B. X.; Pramoda, K. P.; Xu, G. Q.; Goh, S. H. *Adv. Funct. Mater.* **2007**, *17*, 2062.
(7) Lu, K. B.; Grossiord, N.; Koning, C. E.; Miltner, H. E.; Mele, B. V.; Loos, J. *Macromolecules* **2008**, *41*, 8081.
(8) Chen, Q. Y.; Bin, Y. Z.; Matsuo, M. *Macromolecules* **2006**, *39*, 6528.
(9) Zhang, Q. H.; Rastogi, S.; Chen, D. J.; Lippits, D.; Lemstra, P. J. *Carbon* **2006**, *44*, 778.
(10) Liu, T. X.; Phang, I. Y.; Shen, L.; Chow, S. Y.; Zhang, W. D. *Mcromolecules* **2004**, *37*, 256.
(11) McNally, T.; Pötschke, P.; Halley, P; Murphy, M.; Martin, D.; Bell, S. E. J.; Brennan, G. P.; Bein, D.; Lemoine, P.; Quinn, J. P. *Polymer* **2005**, *46*, 8222.
(12) Ganb, M.; Satapathy, B. K.; Thunga, M.; Weidisch, R.; Potschke, P.; Jehnichen, D. *Acta Mater.* **2008**, *56*, 2247.
(13) Xiao, K. Q.; Zhang, L. C.; Zarudi, I. *Compos. Sci. Technol.* **2007**, *67*, 177.
(14) Trijillo, M.; Arnal, M. L.; Muller, A. J. *Macromolecules* **2007**, *40*, 6268.
(15) Li, H. H.; Zhang, X. Q.; Duan, Y. X.; Wang, D. J. *Polymer* **2004**, *45*, 8059.
(16) Haggenmueller, R; Fischer, J. E.; Winey, K. I. *Macromolecules* **2006**, *39*, 2964.
(17) Li, C. Y.; Li, L. Y.; Cai, W. W.; Kodjie, S. L.; Tenneti, K. K. *Adv. Mater.* **2005**, *17*, 1198.
(18) Li, L. Y.; Li, C. Y.; Ni, C. Y. *J. Am. Chem. Soc.* **2006**, *128*, 1692.
(19) Xu, Q.; Yue, J.; Zhang, Z. W.; Chen, Z. M. *Macromolecules* **2007**, *40*, 8821.
(20) Zhang, Q. H.; Lippits, D. R.; Rastogi, S. *Macromolecules* **2006**, *39*, 658.
(21) Ning, N. Y.; Luo, F.; Pan, B. F.; Zhang, Q.; Wang, K.; Fu, Q. *Macromolecules* **2007**, *40*, 8533.
(22) Ning, N. Y.; Luo, F.; Wang, K.; Zhang, Q.; Chen, F.; Du, R.; An, C.; Pan, B. F.; Fu, Q. *J. Phys. Chem. B* **2008**, *112*, 14140.
(23) Guan, Q.; Shen, K. Z.; Li, J.; Zhu, J. *J. Appl. Polym. Sci.* **1996**, *55*, 1797.
(24) Na, B.; Fu, Q. *Polymer* **2001**, *43*, 7367.
(25) Olley, R. H.; Bassett, D. C. *Polymer* **1982**, *23*, 1707.
(26) Mitchell, C. A.; Bahr, J. L.; Arepalli, S.; Tour, J. M.; Krishnamoorti, R. *Macromolecules* **2002**, *35*, 8825.
(27) Kodjie, S. L.; Li, L.; Li, B.; Cai, W.; Li, C. Y.; Keating, M. *J. Macromol. Sci. B Phys.* **2006**, *45*, 231.
(28) Seeger, A.; Freitag, D.; Freidel, F.; Luft, G. *Thermochim. Acta* **2004**, *424*, 175.
(29) Kong, J.; Fan, X.; Qiao, W.; Xie, Y.; Si, Q.; Tang, Y. *Polymer* **2005**, *46*, 7644.
(30) Wunderlich, B.; , *Thermal Analysis*. Academic Press: San Diego, CA, 1990.